Published in final edited form as:
Biomaterials. 2010 January ; 31(3): 420–427. doi:10.1016/j.biomaterials.2009.09.062.

Biological performance of mussel-inspired adhesive in extrahepatic islet transplantation

Carrie E. Brubaker[a,b], **Hermann Kissler**[c], **Ling-jia Wang**[c], **Dixon B. Kaufman**[b,c,‡], and **Phillip B. Messersmith**[a,b,‡,*]

[a] Biomedical Engineering Department, Northwestern University, Evanston, Illinois 60208, USA

[b] Institute for BioNanotechnology in Medicine, Northwestern University, Chicago, Illinois 60611, USA

[c] Department of Surgery, Division of Organ Transplantation, Feinberg School of Medicine, Northwestern University, Chicago, Illinois 60611, USA

Abstract

There is significant need for effective medical adhesives that function reliably on wet tissue surfaces with minimal inflammatory insult. To address these performance characteristics, we have generated a synthetic adhesive biomaterial inspired by the protein glues of marine mussels. In-vivo performance was interrogated in a murine model of extrahepatic syngeneic islet transplantation, as an alternative to standard portal administration. The adhesive precursor polymer consisted of a branched poly (ethylene glycol) (PEG) core, whose endgroups were derivatized with catechol, a functional group abundant in mussel adhesive proteins. Under oxidizing conditions, adhesive hydrogels formed in less than one minute from catechol-derivatized PEG (cPEG) solutions. Upon implantation, the cPEG adhesive elicited minimal acute or chronic inflammatory response in C57BL6 mice, and maintained an intact interface with supporting tissue for up to one year. In-situ cPEG adhesive formation was shown to efficiently immobilize transplanted islets at the epididymal fat pad and external liver surfaces, permitting normoglycemic recovery and graft revascularization. These findings establish the use of synthetic, biologically-inspired adhesives for islet transplantation at extrahepatic sites.

Keywords

Biomimetic material; Tissue adhesive; Islet; Diabetes; Hydrogel; Biocompatibility

1. Introduction

Robust adhesion and cohesive integrity represent valuable characteristics of a medical adhesive, especially for applications requiring long-term performance of the material. However, limitations of currently approved synthetic adhesives include poor adhesion in the presence of biological fluids, sensitization and allergic response, and inflammation [1]. Overcoming these performance deficiencies requires a material that is easily administered in a clinical environment, reliably and durably bonds to target tissue surfaces in a wet environment, has sufficient cohesive strength, and stimulates minimal local or systemic

*Corresponding author. Fax: +1 847 491 4928, philm@northwestern.edu.
‡These investigators are joint senior authors.

inflammatory insult. To generate such a material, we have taken inspiration from the remarkable adhesive capabilities of the marine blue mussel *Mytilus edulis* [2]. Mussel adhesive proteins that comprise the secreted *M. edulis* foot pad are enriched in the post-translationally modified amino acid 3,4-dihydroxy-phenylalanine (DOPA) [3–5]. Subsequent to secretion of the liquid protein precursor, oxidation of the DOPA catechol side chain leads to intermolecular coupling reactions among the mussel adhesive proteins and in-situ hardening of the mussel foot pad [6,7]. Adhesion to the target surface is also mediated by DOPA, in the form of a variety of strong noncovalent and covalent chemical interactions with solid substrates[8]. Motivated by the belief that catechol incorporation into synthetic polymers will enhance wet adhesive properties, we as well as others have investigated catechol-containing linear or branched synthetic polymers as mimics of mussel and other marine adhesives [9–16]. Although in-vitro evaluation of tissue biocompatibility and adhesion have been reported [10,11,13,16,17], in-vivo performance of these candidate medical adhesives has not been investigated. The purpose of this work was to demonstrate mussel-inspired adhesive performance in-vivo, with an emphasis on tissue biocompatibility and integrity of the adhesive/tissue interface.

To this end, biomimetic cPEG adhesive performance was interrogated in a murine animal model of islet transplantation, for the amelioration of diabetes. In humans, type I diabetes mellitus is an autoimmune disease resulting from autoreactive T-lymphocyte-mediated destruction of pancreatic islet beta cells [18]. Select patients can be treated by replacing lost beta cell function through whole islet transplantation. The standard methodology of human clinical islet transplantation was successfully established by the Edmonton protocol, which calls for intrahepatic islet delivery to the liver vasculature via portal vein cannulation [19]. However, islet contact with whole blood results in an instant blood-mediated inflammatory response (IBMIR), characterized by platelet and complement activation, neutrophil and monocyte infiltration, and decreased islet viability [20–22]. Furthermore, activation of liver-resident macrophages (Kupffer cells) initiates release of toxic cytokine mediators IL-1β, IL-6, and TNF-α, as well as reactive oxygen species superoxide, hydrogen peroxide, and nitric oxide, with adverse consequences on islet function [23]. Following treatment according to the Edmonton protocol, these effects may compromise islet engraftment and contribute to a gradual decrease in long-term graft survival [24,25].

As a result, there is significant interest in alternative, extrahepatic tissue sites for experimental and clinical islet transplantation [26,27]. To avoid the functional impairment associated with intrahepatic portal infusion, we propose a new islet transplantation paradigm involving direct immobilization of islets onto intra-abdominal tissue surfaces, using a thin, tissue-adherent conformal hydrogel membrane. This ‘islet sealant’ approach offers the potential advantages of convenient, rapid, and minimally invasive islet transplantation by direct apposition of the islet bolus onto tissue surfaces. Further, the technique avoids the intravascular engraftment site, eliminating IBMIR and other adverse effects of first-pass blood exposure in the liver, while maintaining the capability of rapid islet revascularization and the benefits of direct insulin secretion into the portal circulation. Here, we illustrate the concept using a mussel-inspired adhesive polymer hydrogel in a functional model of murine islet transplantation to the epididymal fat pad and external liver surfaces.

2. Materials and methods

2.1 Synthesis of cPEG mussel-mimetic adhesive precursor

5.0 g four-arm PEG-amine (10 kDa; P4AM-10; SunBio, Anyang City, South Korea) was added to 2:1 chloroform:dimethylformamide. Following dissolution, 0.584 g (3.2 mmol) 3,4-dihydroxyhydrocinnamic acid (DOHA; Fluka, Steinheim, Germany), 0.432 g (3.2 mmol) N-Hydroxybenzotriazole (HOBt; Advanced ChemTech, Louisville, Kentucky), 1.21 g (3.2 mmol) HBTU (Novabiochem, San Diego, California), and 680 μL (4.9 mmol) triethylamine

(Sigma, St. Louis, Missouri) were added to the PEG-amine reagent solution. After 1 hour, the reaction solution was filtered and precipitated in cold anhydrous diethyl ether. The resulting white precipitate was collected and dried overnight under vacuum. The dried product was resuspended in 12 mM HCl, filtered, and transferred to dialysis tubing (3,500 MWCO). Extensive dialysis was carried out in acidic water, pH 3.5 – 4.0. Aqueous dialyzed product was filtered, flash frozen, and lyophilized to yield the purified product. UV spectrometry (Abs_{280}; model U-2010; Hitachi, San Jose, California) confirmed DOHA modification of the PEG reagent, via interpolation of adhesive precursor catechol concentration against a DOPA standard curve. Degree of modification of the PEG starting material by DOHA was determined by ^{1}H-NMR (INOVA 500 MHz; Varian, Palo Alto, California) in deuterated chloroform. cPEG was ethylene oxide gas sterilized (AN74i Anprolene sterilizer; Andersen Sterilizers, Haw River, North Carolina) on a twelve-hour cycle prior to in-vivo use.

2.2 Formation of cPEG adhesive hydrogels

cPEG adhesive precursor was dissolved in 2X phosphate-buffered saline at 300 mg/mL. An equivolume solution of 0.056 M sodium periodate (Sigma) in deionized water was added to induce gelation. Gelation time was determined by inversion method.

2.3 Material-only implantation

Healthy, age-matched male C57BL6 mice (Jackson Laboratories, Bar Harbor, Maine) were anesthetized with nebulized isoflurane (IsoThesia; Butler/Abbott Laboratories, North Chicago, Illinois) and intraperitoneal injection of 2% Avertin (2,2,2-tribromoethanol, Sigma) at 0.3 mg/g body weight, prior to shaving of the abdomen and sterile preparation of the surgical site. The left epididymal fat pad was exposed through midline lower abdominal incision and manipulation of the tissue flap. This thin, well-vascularized tissue is analogous to the omentum of larger mammals and has dimensions on the order of 1.5 × 1.5 cm. Sterile, two-component mixing and adhesive delivery was achieved by a dual-barrel blending connector with mixer device (Micromedics, St Paul, Minnesota) containing sterile-filtered 300 mg/mL cPEG and 0.056 M sodium periodate, respectively. Following topical delivery of approximately 100 μL adhesive, the deposition site was left undisturbed for one minute. The sample site was then manually reinserted into the lower abdominal cavity and the incision closed with double-layer suture. Mice were monitored post-operatively until conscious recovery.

At three days, two weeks, six weeks, and one-year post-implant, the adhesive and associated adipose tissue was surgically removed from anesthetized mice, prior to euthanasia. Samples were fixed overnight in 10% neutral-buffered formalin at 4°C and mounted in paraffin. 4 μm tissue sections were subjected to hematoxylin and eosin (H&E) staining and visualized with standard light microscopy (Axioskop and AxioCam MRc5, with associated Axiovision LE imaging software; Zeiss, Jena, Germany).

These and subsequent animal studies were performed with the approval and supervision of the Northwestern University Animal Care and Use Committee.

2.4 Diabetic induction

Five to seven days prior to transplant surgery, healthy, age-matched male C57BL6 mice were intraperitoneally injected with streptozotocin (Sigma) in 0.9% sodium chloride at 220 mg/kg body weight. Streptozotocin is a nitrosourea glucose analog that is specifically transported into beta cells by the GLUT2 receptor, where cytotoxic DNA alkylation ultimately results in diabetes [28]. Recipient mice were considered diabetic following two non-consecutive days of non-fasting blood glucose measurements ≥300 mg/mL. Blood glucose was analyzed on the One Touch BASIC glucose monitor (Lifescan, Milpitas, California) from whole blood obtained by tail snip.

2.5 Donor islet isolation

Healthy, non-diabetic, age-matched male C57BL6 mice were anesthetized and prepared for surgery as above. The bile duct was clamped at the duodenal junction and cannulated for pancreatic perfusion of 3 mL 0.5 mg/mL cold collagenase (Type XI, from *clostridium histolyticum*; Sigma) in Hank's balanced salt solution (HBSS). Perfused pancreata were incubated at 37°C with occasional agitation to promote tissue degradation. The digested tissue was suspended in HBSS + 10% fetal bovine serum (FBS) and briefly centrifuged. The resultant pellet was resuspended and filtered through sterile mesh to remove bulk tissue matter. Centrifugation of the liquid filtrate yielded the islet-containing tissue pellet, which was subjected to Ficoll dextran discontinuous gradient centrifugation. Isolated islets were hand-picked from the gradient, combined, washed 3x with HBSS + 10% FBS, counted, and cultured until use in CMRL-1066 + 10% FBS, 1% penicillin/streptomycin, and 1% L-glutamine, at 37° C with 5% CO_2.

2.6 Islet transplantation

Streptozotocin-induced diabetic mice were anesthetized and prepared for surgery as above. All recipients were syngeneically transplanted with 150 islets. For islet deposition at the epididymal fat pad or liver surfaces, each 150-islet sample was collected in clamped narrow gauge tubing and briefly centrifuged to compact the islet bolus. The tubing was attached to a constant rate syringe (Hamilton, Reno, Nevada), which permitted controlled islet delivery to the exposed tissue surface following clamp removal. In mice receiving islets at the epididymal fat pad with suture closing (n=7), the fatty tissue was folded over the islet deposition site and immobilized with a single suture. For adhesive mediated islet transplant at the epididymal fat pad (n=8), approximately 100 μL cPEG was applied following islet deposition directly on this tissue surface. The adhesive hydrogel was allowed to cure one minute prior to tissue reinsertion into the lower abdominal cavity. Similarly, islets delivered to the liver lobe surface were immobilized with cPEG adhesive application (n=9). For intrahepatic portal control mice (n=7), the 150-islet bolus was drawn into a 3 mL syringe and slowly injected into the liver vasculature following portal vein exposure and cannulation. Bleeding was controlled with discretionary application of Avitene (microfibrillar collagen hemostat; Davol, Warwick, Rhode Island). In all experimental groups, incision sites were closed with double-layer suture, and mice were monitored post-operatively until conscious recovery.

2.7 Analysis of graft and adhesive performance

Transplanted mouse blood glucose was monitored in whole blood obtained from tail snip using One Touch BASIC glucose monitor. Recipient mice were considered normoglycemic upon non-fasting blood glucose < 200 mg/dL. Recipient weight was simultaneously monitored to confirm normal weight gain and glucose management under fed conditions (data not shown). Intraperitoneal glucose tolerance test (IPGTT) was performed at 105 days post-transplant on recovered, normoglycemic recipients and healthy controls (n=5). Mice were fasted for four hours, and water was removed for the duration of the test. 10% glucose (Hospira, Lake Forest, Illinois) at 2 g/kg body weight was injected intraperitoneally to initiate IPGTT. Blood glucose levels were monitored at baseline (30 and 15 minutes prior to injection) and every fifteen minutes following injection for three hours. The integrated insulin response, defined by area under the blood glucose excursion curve, was calculated using the trapezoidal rule.

At 112 days post-transplant, all groups except intrahepatic portal recipients underwent graft explant survival surgery, for graft analysis and to observe subsequent hyperglycemia. Mice were euthanized following return to the diabetic state. Similarly, one mouse transplanted at the epididymal fat pad with cPEG immobilization underwent graft explant for histological analysis at day 100 post-transplant; this mouse was not included in the intraperitoneal glucose tolerance test. The liver was isolated from intrahepatic portal recipients for histological analysis only, in

a non-survival procedure at the termination of in-vivo studies (day 118). Explanted tissues were fixed overnight in 10% neutral-buffered formalin at 4°C and mounted in paraffin. 4 μm tissue sections were stained with hematoxylin and eosin (H&E) for standard light microscopic visualization. Immunohistochemical triple stain was performed to identify insulin, CD31, and OX-41 epitopes, for the visualization of functional islets, vascular endothelial cells, and macrophages, respectively. Slides were serially treated with guinea pig mouse-reactive anti-swine insulin (1° antibody, 200x, 1 h; Dako, Carpinteria, CA) and FITC-conjugated donkey anti-guinea pig (2° antibody, 200x, 30 min; Jackson ImmunoResearch Laboratories, West Grove, PA); rat anti-mouse CD31 (1° antibody, 100x, 1 hr; Fitzgerald, Concord, MA) and Texas Red-conjugated donkey anti-rat (2° antibody, 200x, 30 min; Jackson ImmunoResearch Laboratories); and mouse-reactive mouse anti-rat OX-41 (1° antibody, 100x, 1 hr; Millipore, Billerica, MA) and AMCA-conjugated goat anti-mouse (2° antibody, 200x, 30 min; Jackson ImmunoResearch Laboratories). Treated slides were visualized using standard fluorescence microscopy and RGB channels combined to generate triple-stain images (Axioskop and AxioCam MRc5, with associated Axiovision LE imaging software, Zeiss, Jena, Germany).

2.8 Statistics

All data are expressed as mean (±SEM). Statistical analysis of experimental groups was performed using one-way analysis of variance (ANOVA) and Tukey's multiple comparisons post-test. Statistical significance was defined as $p < 0.05$. Normal distribution of the data was confirmed by the method of Kolmogorov and Smirnov.

3. Results

3.1 Preparation of the cPEG precursor polymer and cross-linked adhesive hydrogel

To generate the adhesive precursor polymer, an amine-terminated four-arm poly(ethylene glycol) (PEG, 10kDa) was modified with 3,4-dihydroxyhydrocinnamic acid (DOHA) through standard peptide chemistry. The resultant four-arm, catechol-terminated PEG (cPEG) adhesive precursor (Fig. 1a) was synthesized on the multi-gram scale, facilitating its use in animal studies. As determined by ^{1}H-NMR (Supplementary Information, Fig. 1) and UV spectrometry, there was 76% DOHA modification of the PEG starting material, with 0.4 μmol catechol per mg cPEG polymer.

cPEG readily dissolves in relevant aqueous buffers such as phosphate-buffered saline, yielding a free-flowing transparent solution (Fig. 1b). Addition of aqueous sodium periodate solution induces gel formation and material color change from colorless to translucent brown (Fig. 1c). Using the literature as a guide [9], employing optimized cPEG and sodium periodate cross-linker solution concentrations provoked hydrogel formation within twenty to thirty seconds after mixing.

3.2 Evaluation of cPEG adhesive implantation at the murine epididymal fat pad

Healthy, untreated mice received 100–150 μL adhesive, expelled directly from a double barrel syringe mixer/applicator, on the flat surface of the epididymal fat pad. A thin conformal hydrogel membrane formed in under one minute, after which manipulation by gentle depression, folding, and lavage did not interfere with gel integrity or adhesion to the underlying tissue. The adhesive produced no immediate visible inflammation or redness at the deposition site. Following surgery, all mice recovered normally and remained healthy over the course of the study. At three days, two weeks, six weeks, and one year post-implantation, the adhesive/tissue sample was isolated for histological analysis (Fig. 2). In each sample, the adhesive, with uniform pink-purple hue, is attached to and surrounded by epididymal fat pad tissue, whose adipocyte cell membranes are stained in this technique. Little to no inflammatory cell infiltrate is observed at any time point, with little evidence of fibrotic capsule formation over time.

Grossly, at all observed timepoints, the adhesive hydrogel material was visible and present at the original deposition site, and the material-tissue interface was intact. The surrounding adipose tissue was healthy and well-vascularized, and there was no evidence of non-specific post-surgical adhesions.

3.3 Outcome of cPEG-mediated syngeneic islet transplantation

Adhesive-mediated islet transplantation was performed at the epididymal fat pad and on the liver surface. At both sites, the cPEG adhesive formed a visible, translucent, thin hydrogel layer over the affixed islet bolus, resulting in islet entrapment between the adhesive and tissue surface. Two groups of control mice received 150 islets per mouse at the epididymal fat pad (single suture closure, no adhesive), or into the liver via hepatic portal vein cannulation. Islet transplant recipients recovered normally post-surgery.

Blood glucose was monitored for four months following transplantation, as a measure of islet graft performance and adhesive biocompatibility (Fig. 3a). Between mice transplanted at the sutured epididymal fat pad, at the epididymal fat pad with cPEG adhesive immobilization, and via intrahepatic portal infusion, there was no statistical difference in the mean number of days post-transplant upon which normoglycemia was achieved. Islet engraftment to the external liver surface using cPEG adhesive required a significantly longer time to achieve normoglycemia than the three other groups ($p < 0.001$, all cases). Kaplan-Meier survival curves highlight the outcome of islet transplantation for the various groups (Fig. 3b). Mice transplanted at the sutured epididymal fat pad regained normoglycemia at 5.1±1.3 days following surgery (mean±SEM), whereas mice transplanted intrahepatically via portal vein cannulation regained normoglycemia at 7.6±1.1 days. Further, all mice transplanted at the epididymal fat pad with cPEG-immobilized islets achieved normoglycemia, at a mean of 11.5±2.2 days. In the case of islet immobilization on the external liver surface, there was 89% success rate of normoglycemic induction (1 islet graft failure). This experimental group demonstrated a broader range of cure times, with a mean of 50.8±8.5 days.

3.4 Intraperitoneal glucose tolerance test

To assess islet graft response to elevated blood glucose in real time, and to establish prolonged adhesive non-interference with transplanted islet function, an intraperitoneal glucose tolerance test was performed at 105 days post-transplant. Prior to injection, all groups displayed similar baseline blood glucose levels following four-hour fast. Blood glucose levels rose immediately following injection, peaked at 30 minutes in all groups, and fell over time with islet graft response (Fig. 4a). The area under the excursion curve (AUC), also known as the integrated insulin response, was significantly less for the sutured epididymal fat pad group compared to healthy controls. Otherwise, there was no statistical difference in AUC values among the remaining groups (Fig. 4b).

3.5 Graft removal and histological analysis

At 112 days post-transplant, islet grafts with associated adipose tissue were removed from sutured epididymal fat pad and epididymal fat pad with adhesive recipient groups. Similarly, graft explants were collected through partial lobectomy for analysis of cPEG-immobilized islets at the external liver surface. The applied adhesive was visible at the epididymal fat pad and liver surfaces (Fig. 5, top row), and was removed intact with the tissue graft. All mice survived explant surgery, which resulted in immediate hyperglycemia in these two groups as well as the sutured epididymal fat pad control group (Fig. 3a). On day 118, whole organ removal provided tissue samples of intraportally-delivered islets distributed in the liver vasculature. H&E staining of explant samples from all four groups showed intact, rounded islet architecture and direct islet contact with recipient tissue surfaces (Fig. 5, middle row). At the epididymal

fat pad and liver surfaces, cPEG maintained intimate fixation to islets and recipient tissues and induced minimal inflammatory response.

Immunohistochemical triple stain analysis was performed on explant samples, for the identification of insulin-producing functional islets, infiltrating macrophages, and vascular endothelial cells (Fig. 5, bottom row; Supplementary Information, Fig. 2). There was no qualitative difference in intra-islet insulin production (green FITC signal) among the transplant groups. Little to no OX-41 signal indicated minimal macrophage infiltrate, but some non-specific labeling of the cPEG adhesive is observed (disperse blue AMCA signal). In a representative image following minimal islet transplantation at the epididymal fat pad with suture (Fig. 5, bottom row, left panel), OX-41 signal has co-localized with CD31 labeling (Texas red), which identifies intra-islet endothelial cells. Due to limitations of triple-stain immunohistochemistry, CD31 endothelial cell marker signal was restricted in the remaining images; nevertheless, it is possible to identify islet blood supply from histology alone (Fig. 5). More explicitly, Fig. 6 shows H&E-stained, day 100 tissue explant sample from islets transplanted to the epididymal fat pad with cPEG immobilization, in which red erythrocytes are clearly visible in the peri- and intra-islet environment.

4. Discussion

In this study, we prepared an adhesive hydrogel material through chemical cross-linking of a catechol-terminated, PEG-based precursor and demonstrated its application in the murine model of syngeneic minimal islet transplantation. To generate the precursor, 3,4-dihydroxyhydrocinnamic acid (DOHA) was selected as the PEG modifying agent: this DOPA analog contains the catechol moiety essential for cross-linking and interfacial bonding, but lacks the primary amine of the DOPA amino acid, simplifying precursor synthesis and purification. Previous studies of DOPA-terminated branched PEG under similar cross-linking conditions showed that gel formation and color change are due to catechol oxidation and subsequent cross-linking reactions that give rise to a polymer hydrogel network [9]. For future clinical applications, the color change represents a desirable material attribute, as it permits visualization of the applied adhesive on tissue surfaces. Similar cPEG adhesive behavior was observed both in-vitro and in-vivo, even in the presence of biologically relevant fluids such as normal saline and islet culture media, highlighting the rapid, mussel-inspired wet adhesive nature of the cPEG material.

Adhesive performance was first examined in the absence of donor islets, at the epididymal fat pad of male mice. Tissue and cPEG removal surgeries were performed at time points relevant to the acute and chronic inflammatory response, following which explant histology confirmed minimal adhesive-stimulated inflammation. The persistence of cPEG adhesive interface with the epididymal fat pad, extending to one year, underscores the material's utility in adhesive applications requiring prolonged performance. The intimate interface between cPEG hydrogel and tissue likely reflects the presence of covalent bonds between the two, formed during solidification of the adhesive. It was previously shown that the *o*-quinone group – a reactive, oxidized form of the catechol moiety that forms in the presence of periodate – covalently couples with primary amines [6–8]. In addition, we surmise that *o*-quinone will also be reactive toward other nucleophiles such as thiols and imidazoles, resulting in broad reactivity toward residues found in ECM proteins of tissues. Such reactions likely form the basis of the continuous, intact adhesive/tissue interface observed in this study.

Islets are highly sensitive to chemical and physical insults; cPEG-mediated minimal islet transplantation into streptozotocin-induced diabetic mice therefore represents a much more stringent test of material biocompatibility. We hypothesized that rapid, in-situ adhesive gelation would facilitate islet immobilization on the surface of alternative transplant tissue

sites. This approach is minimally invasive to both islets and the recipient tissue and is best implemented on a highly vascular tissue, to allow rapid donor islet revascularization. In this study, we selected the epididymal fat pad and the external liver surface as candidate extrahepatic transplant sites. The epididymal fat pad is an easily-accessed, flexible adipose tissue flap chosen in light of previous syngeneic [29,30] and allogeneic [31] islet transplant studies at this site, whereas the liver surface represents a novel, previously untested site and the one most comparable to established intrahepatic islet delivery. The sutured epididymal fat pad and intrahepatic sites were investigated as relevant controls. All experiments were performed in a syngeneic mouse model, in which the donor and recipient mice were genetically identical. That is, the experiment was designed to isolate the adhesive's influence on transplanted islet function without confounding by specific immune processes such as acute rejection.

With the exception of mice transplanted at the external liver surface, no significant variation in mean time to normoglycemia was observed among transplanted groups. This result indicates that the cPEG material does not interfere with islet engraftment to the recipient epididymal fat pad surface. Further, all transplanted groups performed similarly in the intraperitoneal glucose tolerance test. IPGTT outcomes show that islet function in adhesive-mediated groups was comparable to function in healthy mice and in the clinically-relevant intrahepatic portal transplant site. This suggests that following normoglycemic recovery, the cPEG adhesive does not interfere with islets' real-time blood glucose sensing and insulin response. The adhesive-mediated approach may represent a viable alternative to more invasive and time-consuming epididymal fat pad suturing or intrahepatic portal delivery techniques.

Mean recovery time was significantly longer in mice transplanted with adhesive-immobilized islets at the liver surface. However, following recovery, this group performed similarly to other transplanted groups, including the epididymal fat pad with adhesive group. This may be attributed to recipient tissue architecture and surface characteristics, as opposed to limitations of the cPEG adhesive itself. Whereas the epididymal fat pad is a thin, flat tissue surface, the liver lobe is bulky and convex. Our observations with adhesive application on the external surface of the liver indicated that application of the viscous adhesive may have displaced some islets away from the deposition site; such islets are not expected to adhere to the tissue surface and may ultimately be lost into the intraperitoneal space. Given that the current study employed a minimal islet number (150), loss of islets from the implant site may result in delayed recovery time. We are currently investigating a spray applicator that may allow us to overcome this performance limitation.

At the conclusion of in-vivo studies, immediate return to hyperglycemia following survival graft explant surgery confirmed that transplanted islets were responsible for diabetes reversal and ongoing normoglycemic maintenance. In the intrahepatic portal control group, widespread diffusion of islets in the liver vasculature renders partial lobectomy ineffective for removing all transplanted islets, and the essential nature of liver function to survival precluded whole liver organ removal. In this group it was therefore not possible to confirm the role of transplanted islets in normoglycemic recovery through whole organ explant surgery. Nevertheless, this tissue, with embolized islets, was obtained for histological analysis and comparison to other transplant sites. At each transplant site, islets were present and intact, with obvious blood supply. Islet graft histology confirmed observations from the adhesive-only implant studies: at the site of deposition, the cPEG adhesive induced little to no inflammatory response at either the recipient tissue surface or the transplanted islet bolus.

Immunohistochemical analysis confirmed healthy islet function at the time of graft removal and further demonstrated cPEG adhesive compatibility with transplanted islets and recipient tissues. Nearly total absence of infiltrating macrophages in cPEG-containing samples

supported histological observations of minimal adhesive-stimulated inflammatory cell infiltration. Observed diabetic recovery and ongoing normoglycemic control correlated with evidence of islet insulin production and revascularization, and indicated that adhesive immobilization does not interfere with these processes. In fact, this type of fixation may be vital to islet function, as islets freely transplanted in the intraperitoneal space are subject to limited revascularization/reinnervation and poor blood glucose sensing [32]. In our approach, the adhesive facilitated direct contact between islets and the recipient tissue surface, which may be advantageous to local reestablishment of islet vascularization. Indeed, the most probable origin of vascular infiltration is from this tissue surface, as the cPEG hydrogel forms a dense, long-lasting, and likely impenetrable barrier to cellular migration from the intraperitoneal cavity.

For the present and other envisioned applications, rapid cPEG cross-linking and tissue adhesion under physiologic conditions represent essential material characteristics. Though its robust wet/dry adhesive capabilities were inspired by DOPA catechol reactivity in mussel adhesive proteins, the material's PEG component also plays an important role in adhesive performance in the abdominal space. PEG-based materials have been utilized as synthetic islet immunoisolation barriers, shielding treated islets from elements of the host immune response [33–36]. However, islet encapsulation for the purpose of immunoisolation does not fully exclude low molecular weight inflammatory cytokines, while creating a physical barrier to revascularization and insulin secretion from entrapped islets [37,38]. Rather than immunoisolation, the primary role of the cPEG adhesive in our method is to facilitate the direct apposition of islets to target recipient tissue surfaces. Interestingly, the free surface of solidified cPEG hydrogel is minimally adhesive to nearby tissues, as demonstrated by the complete absence of non-specific post-surgical adhesions in our in-vivo studies, even at the interface between the adhesive-coated liver surface and the abdominal wall. This attribute of cPEG hydrogels is likely a result of high PEG content and is favorable for use in the intraperitoneal cavity, given that non-specific adhesions to neighboring tissues or to the inner abdominal wall should be avoided.

5. Conclusions

This study provided valuable insight into the in-vivo performance of mussel-mimetic cPEG hydrogel in the context of islet transplantation in mice. This cPEG adhesive provoked minimal inflammatory response and did not perturb islet architecture or glucose management, permitting a unique approach to murine islet transplantation through direct immobilization onto two-dimensional recipient tissue surfaces. The successful use of tissue-adherent hydrogel to immobilize islets onto the surface of extrahepatic tissues such as the liver and the epididymal fat pad overcomes disadvantages of existing islet transplantation techniques and supports broader investigation of the cPEG adhesive in islet transplantation and other surgical and biomedical applications.

Supplementary Material

Refer to Web version on PubMed Central for supplementary material.

Acknowledgments

This study was supported by National Institutes of Health grants EB003806 and DE014193. C.E.B. acknowledges the Northwestern University Regenerative Medicine Training Program for support (NIH DA022881). We thank Dr. Bruce Lee for discussions regarding cPEG synthesis and Nicholas Talarico of the Pathology Core Facility, Robert H. Lurie Cancer Center, Northwestern University, for his assistance with histology and immunohistochemistry. Dr. Harsha Kulkarni is acknowledged for assistance with mouse monitoring and care.

References

1. Spotnitz WD, Burks S. Hemostats, sealants, and adhesives: components of the surgical toolbox. Transfusion (Paris) 2008;48:1502–16.
2. Waite JH. Adhesion à la moule. Integr Comp Biol 2002;42:1172–80.
3. Waite JH, Tanzer ML. Polyphenolic substance of Mytilus edulis: Novel adhesive containing L-Dopa and hydroxyproline. Science 1981;212:1038–40. [PubMed: 17779975]
4. Papov VV, Diamond TV, Biemann K, Waite JH. Hydroxyarginine-containing polyphenolic proteins in the adhesive plaques of the marine mussel Mytilus edulis. J Biol Chem 1995;270:20183–92. [PubMed: 7650037]
5. Waite JH, Qin X. Polyphosphoprotein from the adhesive pads of Mytilus edulis. Biochemistry 2001;40:2887–93. [PubMed: 11258900]
6. Burzio LA, Waite JH. Cross-linking in adhesive quinoproteins: studies with model decapeptides. Biochemistry 2000;39:11147–53. [PubMed: 10998254]
7. Yu ME, Hwang JY, Deming TJ. Role of L-3,4-dihydroxyphenylalanine in mussel adhesive proteins. J Am Chem Soc 1999;121:5825–6.
8. Lee H, Scherer NF, Messersmith PB. Single-molecule mechanics of mussel adhesion. Proc Natl Acad Sci U S A 2006;103:12999–13003. [PubMed: 16920796]
9. Lee BP, Dalsin JL, Messersmith PB. Synthesis and gelation of DOPA-modified poly(ethylene glycol) hydrogels. Biomacromolecules 2002;3:1038–47. [PubMed: 12217051]
10. Shao H, Bachus KN, Stewart RJ. A water-borne adhesive modeled after the sandcastle glue of P. californica. Macromol Biosci 2009;9:464–71. [PubMed: 19040222]
11. Wang J, Liu C, Lu X, Yin M. Co-polypeptides of 3,4-dihydroxyphenylalanine and l-lysine to mimic marine adhesive protein. Biomaterials 2007;28:3456–68. [PubMed: 17475323]
12. Westwood G, Horton TN, Wilker JJ. Simplified polymer mimics of cross-linking adhesive proteins. Macromolecules 2007;40:3960–4.
13. Yin M, Yuan Y, Liu C, Wang J. Development of mussel adhesive polypeptide mimics coating for in-situ inducing re-endothelialization of intravascular stent devices. Biomaterials 2009;30:2764–73. [PubMed: 19223071]
14. Yu M, Deming TJ. Synthetic polypeptide mimics of marine adhesives. Macromolecules 1998;31:4739–45. [PubMed: 9680407]
15. Hu B-H, Messersmith PB. Rational design of transglutaminase substrate peptides for rapid enzymatic formation of hydrogels. J Am Chem Soc 2003;125:14298–9. [PubMed: 14624577]
16. Tatehata H, Mochizuki A, Kawashima T, Yamashita S, Yamamoto H. Model polypeptide of mussel adhesive protein. I. Synthesis and adhesive studies of sequential polypeptides (X-Tyr-Lys)(n) and (Y-Lys)(n). J Appl Polym Sci 2000;76:929–37.
17. Burke SA, Ritter Jones M, Lee BP, Messersmith PB. Thermal gelation and tissue adhesion of biomimetic hydrogels. Biomed Mater 2007;2:203–10. [PubMed: 18458476]
18. Notkins AL. Immunologic and genetic factors in type 1 diabetes. J Biol Chem 2002;277:43545–8. [PubMed: 12270944]
19. Shapiro AM, Lakey JR, Ryan EA, Korbutt GS, Toth E, Warnock GL, et al. Islet transplantation in seven patients with type 1 diabetes mellitus using a glucocorticoid-free immunosuppressive regimen. N Engl J Med 2000;343:230–8. [PubMed: 10911004]
20. van der Windt DJ, Bottino R, Casu A, Campanile N, Cooper DK. Rapid loss of intraportally transplanted islets: an overview of pathophysiology and preventive strategies. Xenotransplantation 2007;14:288–97. [PubMed: 17669170]
21. Moberg L, Korsgren O, Nilsson B. Neutrophilic granulocytes are the predominant cell type infiltrating pancreatic islets in contact with ABO-compatible blood. Clin Exp Immunol 2005;142:125–31. [PubMed: 16178866]
22. Bennet W, Groth CG, Larsson R, Nilsson B, Korsgren O. Isolated human islets trigger an instant blood mediated inflammatory reaction: implications for intraportal islet transplantation as a treatment for patients with type 1 diabetes. Ups J Med Sci 2000;105:125–33. [PubMed: 11095109]

23. Barshes NR, Wyllie S, Goss JA. Inflammation-mediated dysfunction and apoptosis in pancreatic islet transplantation: implications for intrahepatic grafts. J Leukoc Biol 2005;77:587–97. [PubMed: 15728243]
24. Shapiro AM, Ricordi C, Hering BJ, Auchincloss H, Lindblad R, Robertson RP, et al. International trial of the Edmonton protocol for islet transplantation. N Engl J Med 2006;355:1318–30. [PubMed: 17005949]
25. Ryan EA, Paty BW, Senior PA, Bigam D, Alfadhli E, Kneteman NM, et al. Five-year follow-up after clinical islet transplantation. Diabetes 2005;54:2060–9. [PubMed: 15983207]
26. van der Windt DJ, Echeverri GJ, Ijzermans JN, Cooper DK. The choice of anatomical site for islet transplantation. Cell Transplant 2008;17:1005–14. [PubMed: 19177837]
27. Merani S, Toso C, Emamaullee J, Shapiro AM. Optimal implantation site for pancreatic islet transplantation. Br J Surg 2008;95:1449–61. [PubMed: 18991254]
28. Elsner M, Guldbakke B, Tiedge M, Munday R, Lenzen S. Relative importance of transport and alkylation for pancreatic beta-cell toxicity of streptozotocin. Diabetologia 2000;43:1528–33. [PubMed: 11151762]
29. Chen X, Zhang X, Larson C, Chen F, Kissler H, Kaufman DB. The epididymal fat pad as a transplant site for minimal islet mass. Transplantation 2007;84:122–5. [PubMed: 17627248]
30. Dufour JM, Rajotte RV, Zimmerman M, Rezania A, Kin T, Dixon DE, et al. Development of an ectopic site for islet transplantation, using biodegradable scaffolds. Tissue Eng 2005;11:1323–31. [PubMed: 16259588]
31. Chen XJ, Zhang XM, Larson CS, Baker MS, Kaufman DB. In vivo bioluminescence imaging of transplanted islets and early detection of graft rejection. Transplantation 2006;81:1421–7. [PubMed: 16732180]
32. Fritschy WM, van Straaten JF, de Vos P, Strubbe JH, Wolters GH, van Schilfgaarde R. The efficacy of intraperitoneal pancreatic islet isografts in the reversal of diabetes in rats. Transplantation 1991;52:777–83. [PubMed: 1835193]
33. Cruise GM, Hegre OD, Lamberti FV, Hager SR, Hill R, Scharp DS, et al. In vitro and in vivo performance of porcine islets encapsulated in interfacially photopolymerized poly(ethylene glycol) diacrylate membranes. Cell Transplant 1999;8:293–306. [PubMed: 10442742]
34. Cheung CY, Anseth KS. Synthesis of immunoisolation barriers that provide localized immunosuppression for encapsulated pancreatic islets. Bioconjug Chem 2006;17:1036–42. [PubMed: 16848413]
35. Yun Lee D, Hee Nam J, Byun Y. Functional and histological evaluation of transplanted pancreatic islets immunoprotected by PEGylation and cyclosporine for 1 year. Biomaterials 2007;28:1957–66. [PubMed: 17188350]
36. Wilson JT, Cui WX, Chaikof EL. Layer-by-layer assembly of a conformal nanothin PEG coating for intraportal islet transplantation. Nano Lett 2008;8:1940–8. [PubMed: 18547122]
37. de Groot M, Schuurs TA, van Schilfgaarde R. Causes of limited survival of microencapsulated pancreatic islet grafts. J Surg Res 2004;121:141–50. [PubMed: 15313388]
38. Weber LM, Lopez CG, Anseth KS. Effects of PEG hydrogel crosslinking density on protein diffusion and encapsulated islet survival and function. J Biomed Mater Res A 2008;90:720–9. [PubMed: 18570315]

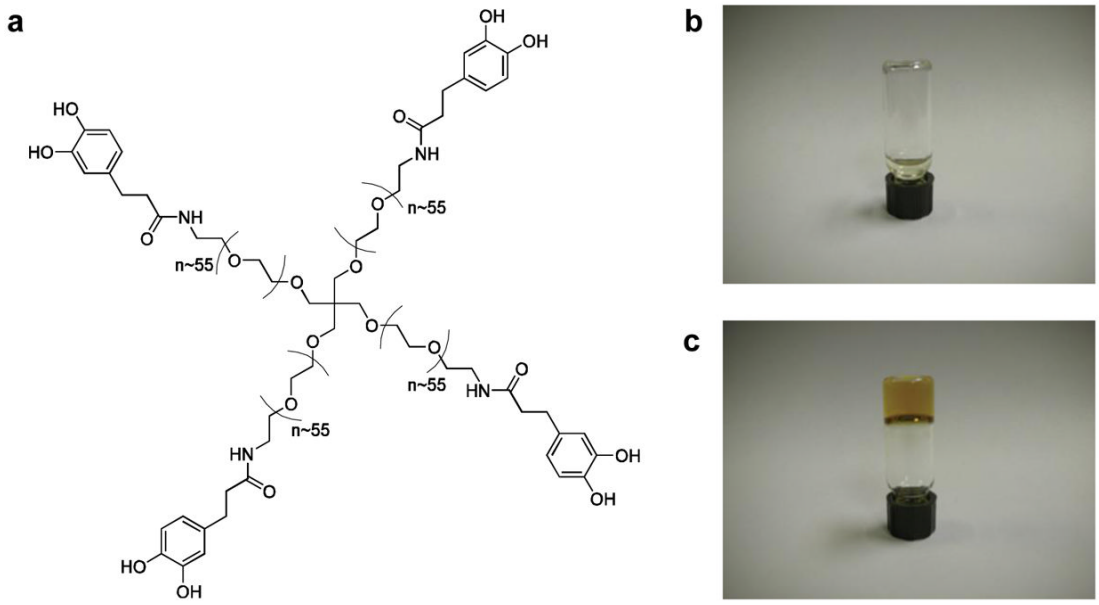

Fig. 1.

Structure and gelation of the catechol-terminated cPEG adhesive precursor. (a) Chemical structure of cPEG adhesive precursor. Photographs of precursor solution in phosphate-buffered saline before (b) and after (c) addition of aqueous sodium periodate solution; gel formation occurred within twenty to thirty seconds.

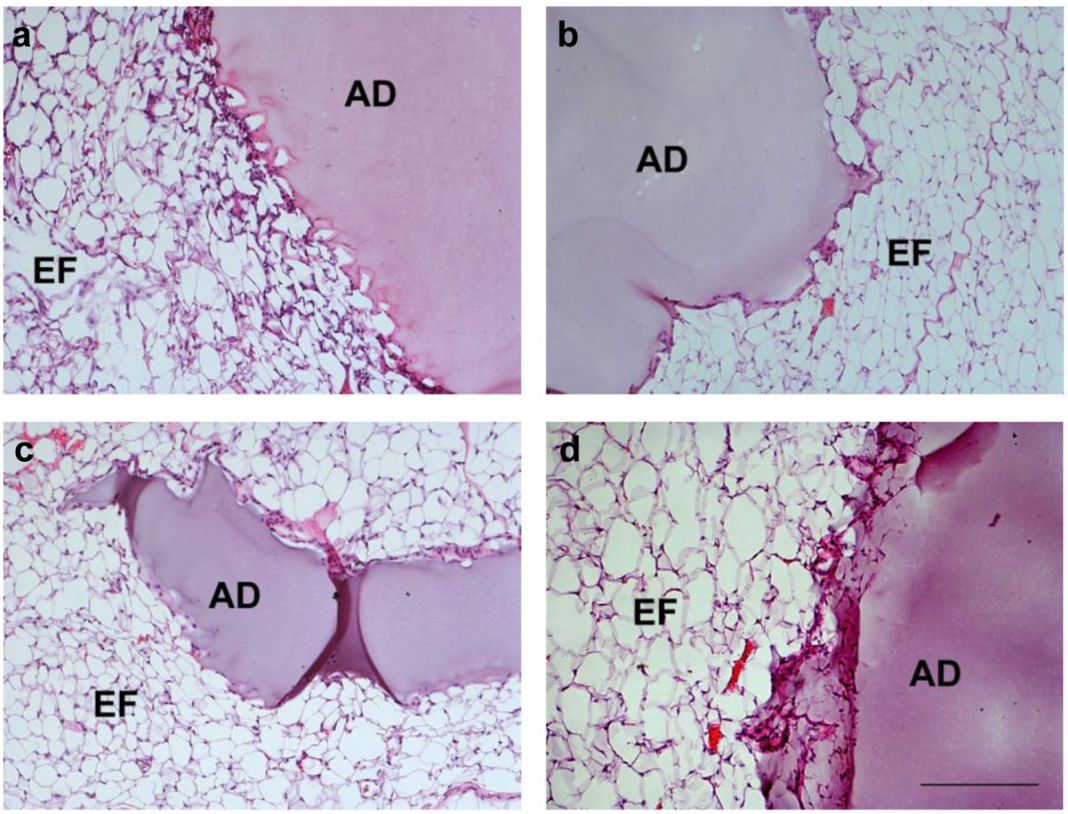

Fig. 2.

Representative light micrographs of hematoxylin and eosin (H&E)-stained cPEG adhesive and mouse epididymal fat pad tissue samples removed at three days (a), two weeks (b), six weeks (c), and one year (d) after material-only implantation. Adhesive, AD; epididymal fat tissue, EF. All images, scale bar: 200 μm.

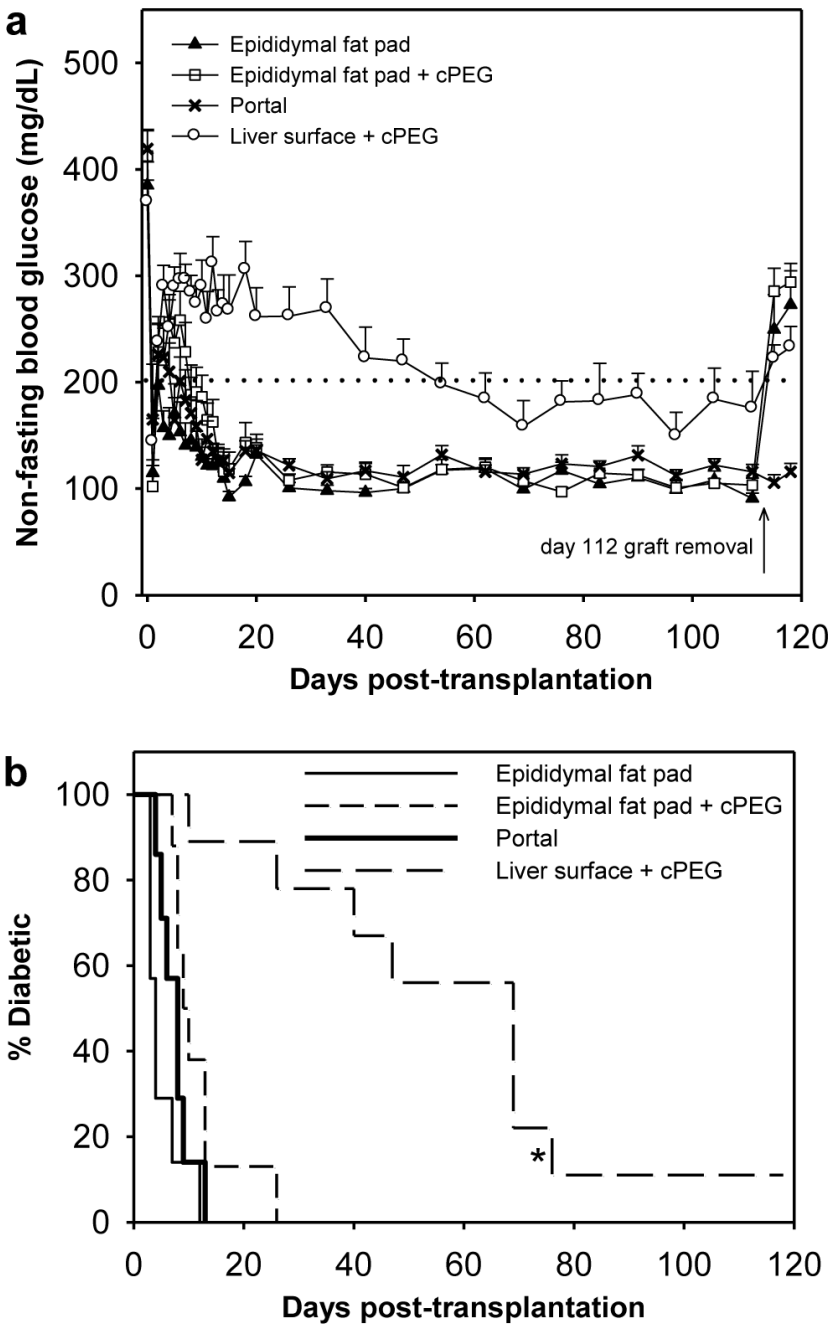

Fig. 3.

Normoglycemic recovery following cPEG adhesive-mediated minimal islet transplantation. (a) Mean non-fasting blood glucose from day 0 (day of transplantation) to day 118 (day of euthanasia), in mice that received 150 islets at the sutured epididymal fat pad (▲, n=7); at the epididymal fat pad with adhesive immobilization (□, n=8); via intrahepatic portal delivery (**x**, n=7); and at the liver surface with adhesive immobilization (○, n=9). Normoglycemia is defined as non-fasting blood glucose < 200 mg/dL (dotted line). Error bars represent standard error of the mean. (b) Percentage of diabetic recipients remaining within each group as a function of time, following 150-islet transplantation at the sutured epididymal fat pad (solid fine line), at the epididymal fat pad with adhesive immobilization (short dashed line), via

intrahepatic portal delivery (solid bold line), and at the liver surface with adhesive immobilization (long dashed line). Asterisk (*) indicates statistical significance in the mean number of days to cure (with n=8) compared to all other groups ($p < 0.001$).

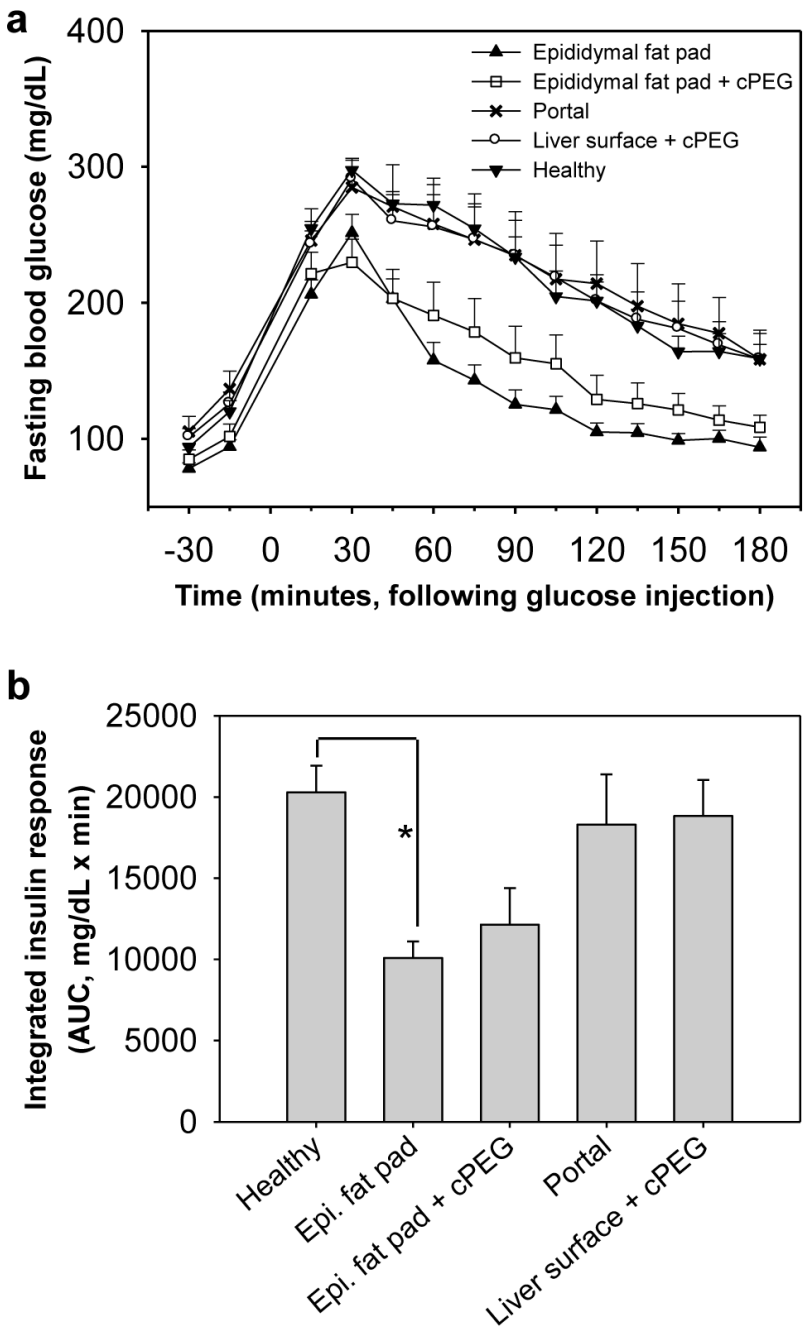

Fig. 4.

Real-time graft performance in intraperitoneal glucose tolerance test. (a) Mean fasting blood glucose over time, following intraperitoneal injection of 10% glucose. Test groups were composed of normoglycemic mice previously transplanted at the sutured epididymal fat pad (▲, n=7); at the epididymal fat pad with adhesive immobilization (□, n=8); via intrahepatic portal delivery (**x**, n=7); at the liver surface with adhesive immobilization (○, n=8); as well as healthy untreated control mice (▼, n=5). (b) Integrated insulin response to intraperitoneal glucose injection, calculated by group. Asterisk (*) indicates statistical difference in mean area under blood glucose excursion curve (AUC) between the sutured epididymal fat pad and healthy control groups ($p < 0.05$).

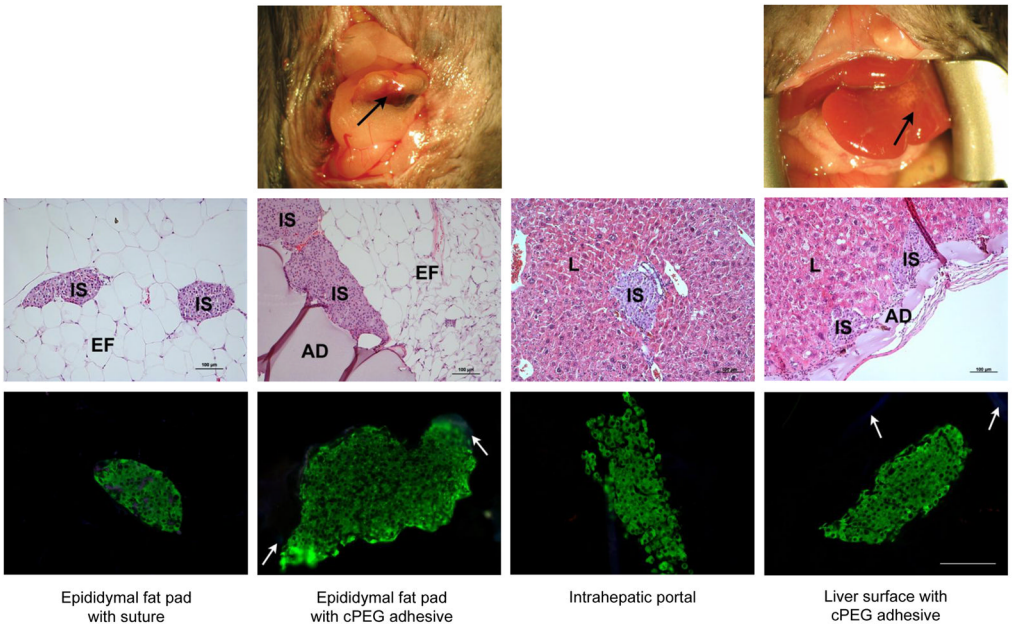

Fig. 5.

Analysis of islet graft and cPEG adhesive explants. Top row: photographic images of the site of cPEG adhesive-mediated 150-islet transplantation at the epididymal fat pad and liver surface, immediately prior to graft explant on day 112. Immobilized islet bolus is visible on the external liver surface. Black arrows, cPEG adhesive. Middle row: representative light micrographs of hematoxylin and eosin (H&E)-stained graft explants. Adhesive, AD; islet, IS; epididymal fat tissue, EF; liver tissue, L. Scale bars: 100 μm. Bottom row: representative fluorescent micrographs of immunohistochemical triple-stain of graft explants. Insulin, green; OX-41 (macrophage marker), blue; CD31 (endothelial cell marker), red. White arrows, non-specific cPEG labeling. All images, scale bar: 100 μm.

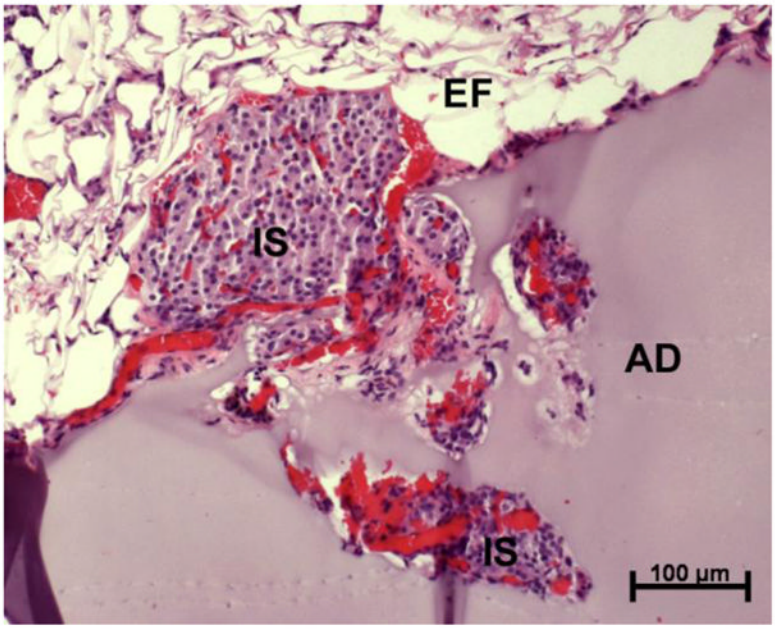

Fig. 6.
Light micrograph of hematoxylin and eosin (H&E)-stained tissue explant demonstrating cPEG adhesive-mediated islet attachment and revascularization at the epididymal fat pad surface. Graft was removed at day 100 following transplantation. Adhesive, AD; islet, IS; epididymal fat tissue, EF.